Classification of targets using optimized ISAR Euler imagery

C. Baird*[a], W. T. Kersey[a], R. Giles[a], W. E. Nixon[b]

[a]University of Massachusetts Lowell, Submillimeter-Wave Technology Laboratory(STL)
175 Cabot Street, Lowell, Massachusetts 01854

[b]U.S. Army National Ground Intelligence Center (NGIC)
2055 Boulders Road, Charlottesville, VA 22911

ABSTRACT

Various approaches exist to enable target classification through a decomposition of the polarimetric scattering matrix. Specifically, the Euler decomposition attempts to express the target scattering properties through more physically relevant parameters. Target classification in general has been limited by signature variability and the saturation of images by non-persistent scatterers.[1] The Euler decomposition is sensitive to additional parameter ambiguities.[2] It will be demonstrated how undesirable ambiguities may be identified and mitigated. Through the analysis of polarimetric ISAR signatures obtained in compact radar ranges at the University of Massachusetts Lowell Submillimeter Technology Laboratory (STL)[3,4,5,6] and the U.S. Army National Ground Intelligence Center (NGIC), the cause of non-persistent scatters will be investigated. A proper characterization of non-persistence should lead to better optimization of the Euler decomposition, and thus improve target classification.

Keywords: HRR, Ka-Band, polarimetric, signature, ISAR, Euler

1. INTRODUCTION

The reproducibility of high-resolution target signatures, specifically of main battle tanks (MBT) was originally investigated under a project[4,6] sponsored and supervised by the U.S. Army National Ground Intelligence Center (NGIC). The project involved obtaining full-polarimetric Ka-band radar signatures at Eglin AFB as well as obtaining equivalent scaled signatures in submillimeter-wave compact radar ranges. The scaled signatures were acquired using exact 1/16th scale replicas fabricated through the ERADS program and imaged in the compact radar ranges of NGIC and of the University of Massachusetts Lowell Submillimeter Technology Laboratory (STL). Through NGIC's sponsorship, the signatures were evaluated to improve methods for target classification. The endeavor to optimize Ka-band ISAR imagery in Euler parameter space in order to improve classification is a continuation of the original project.

2. ISAR EULER IMAGERY

A traditional Inverse Synthetic Aperture Radar (ISAR) setup sweeps a band of frequencies and a swath of angles, coherently measuring the backscattered radiation for each polarization possibility. A two-dimensional Fourier transform converts the data into a spatial image of the target's reflectivity, where each spatial resolution cell contains the full-polarimetric response of the targets in that cell as represented in the Scattering matrix *S*,

$$S = \begin{bmatrix} S_{hh} & S_{hv} \\ S_{vh} & S_{vv} \end{bmatrix} \tag{1}$$

* Correspondence: Email: Christopher_Baird@student.uml.edu; Telephone: (978)934-1300; Fax: (978) 452-3333
SPIE #6210-09

Report Documentation Page

Form Approved
OMB No. 0704-0188

1. REPORT DATE	2. REPORT TYPE	3. DATES COVERED
MAY 2006		**00-00-2006 to 00-00-2006**

4. TITLE AND SUBTITLE	5a. CONTRACT NUMBER
Classification of targets using optimized ISAR Euler imagery	5b. GRANT NUMBER
	5c. PROGRAM ELEMENT NUMBER
6. AUTHOR(S)	5d. PROJECT NUMBER
	5e. TASK NUMBER
	5f. WORK UNIT NUMBER
7. PERFORMING ORGANIZATION NAME(S) AND ADDRESS(ES) **University of Massachusetts Lowell,Submillimeter-Wave Technology Laboratory,175 Cabot Street,Lowell,MA,01854**	8. PERFORMING ORGANIZATION REPORT NUMBER
9. SPONSORING/MONITORING AGENCY NAME(S) AND ADDRESS(ES)	10. SPONSOR/MONITOR'S ACRONYM(S)
	11. SPONSOR/MONITOR'S REPORT NUMBER(S)

12. DISTRIBUTION/AVAILABILITY STATEMENT
Approved for public release; distribution unlimited

13. SUPPLEMENTARY NOTES

14. ABSTRACT

15. SUBJECT TERMS

16. SECURITY CLASSIFICATION OF:			17. LIMITATION OF ABSTRACT	18. NUMBER OF PAGES	19a. NAME OF RESPONSIBLE PERSON
a. REPORT	b. ABSTRACT	c. THIS PAGE			
unclassified	**unclassified**	**unclassified**		**11**	

where, S_{vh} for example, represents the complex backscattering measured when horizontally-polarized waves are transmitted and vertically-polarized waves are received. Often, the phase information is neglected and the magnitude images are used as the final form. Correlation studies have previously been pursued in such a way under the support of NGIC[6]. However, several decomposition techniques exist to transform the scattering matrix values into more useful parameters. Among them, the Euler decomposition developed chiefly by Kennaugh[8] and Huynen[9] transforms the matrix into phenomenological variables, and thus leads to spatial images of the target's Euler properties. Autonne[5] showed that the complex symmetric matrix S can be diagonalized by applying a consimilarity transform (Equation 2), where the transform matrix U is constructed from the eigenvectors satisfying the conjugate eigenvalue equation (Equation 3).

$$S_D = U^T S U \tag{2}$$

$$S \boldsymbol{x}_i = \lambda_i \boldsymbol{x}_i^* \tag{3}$$

The Euler parameters are then defined in terms of the diagonal scattering matrix S_D (Equation 4) and the transform matrix U (Equation 5) where m denotes maximum reflectivity, ψ denotes the object orientation angle, τ is the symmetry angle, υ is the bounce angle, and γ represents the polarizability angle.

$$S_D = \begin{bmatrix} m e^{i2\nu} & 0 \\ 0 & m\tan^2(\gamma) e^{-i2\nu} \end{bmatrix} \tag{4}$$

$$U = \begin{bmatrix} \cos(\psi)\cos(\tau) - i\sin(\psi)\sin(\tau) & -\sin(\psi)\cos(\tau) + i\cos(\psi)\sin(\tau) \\ \sin(\psi)\cos(\tau) + i\cos(\psi)\sin(\tau) & \cos(\psi)\cos(\tau) + i\sin(\psi)\sin(\tau) \end{bmatrix} \tag{5}$$

Because these relations establish an inverse problem that must be solved in order to be useful in practice, several ambiguities can arise. In order to meaningfully represent the corresponding physical properties, each Euler parameter must be derived from the scattering matrix in a way that minimizes ambiguities. This derivation is best approached in the power representation of the scattering properties, as contained in the Kennaugh matrix. The Kennaugh matrix is derived from the Scattering matrix in the same way the Mueller matrix is derived from the Jones matrix in optical scattering, with the essential difference being that the Kennaugh matrix is represented in the Back Scattering Alignment (BSA) coordinate system. When a meaningless overall phase factor g is removed from the scattering matrix S and reciprocity is assumed, S can be compactly represented by the five real parameters *a, b, c, d, f,*

$$S = e^{ig}\begin{bmatrix} a e^{ib} & c \\ c & d e^{if} \end{bmatrix} \quad \text{where} \quad \begin{array}{l} a = |S_{hh}|,\ b = \mathrm{Arg}(S_{hh}) - \mathrm{Arg}(S_{hv}),\ c = |S_{hv}|,\ d = |S_{vv}|, \\ f = \mathrm{Arg}(S_{vv}) - \mathrm{Arg}(S_{hv}),\ \ g = \mathrm{Arg}(S_{hv}). \end{array} \tag{6}$$

The Kennaugh matrix K which corresponds to a certain scattering matrix S is found by solving for electric field strengths. When the scattering matrix has the form in Equation 6, the corresponding Kennaugh matrix can then be expressed in terms of these known real parameters (Equation 7).

$$K = \begin{bmatrix} \frac{1}{2}(a^2 + 2c^2 + d^2) & \frac{1}{2}(a^2 - d^2) & ac\cos b + d\cos f & ac\sin b - cd\sin f \\ \frac{1}{2}(a^2 - d^2) & \frac{1}{2}(a^2 - 2c^2 + d^2) & ac\cos b - cd\cos f & ac\sin b + cd\sin f \\ ac\cos b + cd\cos f & ac\cos b - cd\cos f & c^2 + ad\cos(b-f) & ad\sin(b-f) \\ ac\sin b - cd\sin f & ac\sin b + cd\sin f & ad\sin(b-f) & c^2 - ad\cos(b-f) \end{bmatrix} \tag{7}$$

To simplify notation, new variables are defined in terms of the known parameters (Equation 8).

$$K=\begin{bmatrix} A_0+B_0 & C_\psi & H_\psi & F \\ C_\psi & A_0+B_\psi & E_\psi & G_\psi \\ H_\psi & E_\psi & A_0-B_\psi & D_\psi \\ F & G_\psi & D_\psi & -A_0+B_0 \end{bmatrix} \tag{8}$$

By applying back rotations one by one, the dependence of K on the angles ψ, τ, and υ can be removed. Through this process, the angles ψ (Equation 9), τ (Equation 10), and υ (Equation 11) can be determined by requiring the subsequent matrices to be stepwise diagonalized, as discussed more thoroughly by Huynen[10].

$$\psi=\tan^{-1}\left(\frac{-C_\psi+\sqrt{C_\psi^2+H_\psi^2}}{H_\psi}\right) \tag{9}$$

$$\tau=\frac{1}{2}\tan^{-1}\left(\frac{F_\psi}{C_\psi\cos(2\psi)+H_\psi\sin(2\psi)}\right) \tag{10}$$

$$\nu=\frac{1}{2}\tan^{-1}\left(\frac{B-A_0+\sqrt{(B-A_0)^2+(D\cos(2\tau)-E\sin(2\tau))^2}}{D\cos(2\tau)-E\sin(2\tau)}\right) \tag{11}$$

where
$$B=B_\psi\cos(4\psi)+E_\psi\sin(4\psi)$$
$$E=E_\psi\cos(4\psi)-B_\psi\sin(4\psi)$$
$$D=D_\psi\cos(2\psi)-G_\psi\sin(2\psi)$$

The remaining partially-diagonalized Kennaugh matrix K''' has a form that is independent of ψ, τ, and υ,

$$K'''=m^2\begin{bmatrix} \frac{1}{2}(1+\tan^4(\gamma)) & \frac{1}{2}(1-\tan^4(\gamma)) & 0 & 0 \\ \frac{1}{2}(1-\tan^4(\gamma)) & \frac{1}{2}(1+\tan^4(\gamma)) & 0 & 0 \\ 0 & 0 & \tan^2(\gamma) & 0 \\ 0 & 0 & 0 & -\tan^2(\gamma) \end{bmatrix} \tag{12}$$

which can be solved for the remaining Euler parameters m (Equation 13) and γ (Equation 14).

$$m=\sqrt{A_0+B_0+\sqrt{C_\psi^2+F_\psi^2+H_\psi^2}} \tag{13}$$

$$\gamma=\tan^{-1}\left[\frac{A_0+B_0-\sqrt{C_\psi^2+H_\psi^2+F_\psi^2}}{A_0+B_0+\sqrt{C_\psi^2+H_\psi^2+F_\psi^2}}\right]^{1/4} \tag{14}$$

Thus, explicit transformation equations have been derived for all of the Euler parameters in a way that minimizes ambiguities. Using these equations, the full-polarimetric ISAR images of a target can be transformed into spatial images of a target's maximum reflectivity, orientation, symmetry, bounce properties, and polarizability.

3. REDEFINING UNAVOIDABLE AMBIGUITIES

Unavoidable ambiguities arise in the Euler transform process when multiple distinct sets of Euler parameters map to the same scattering matrix. The existence of such ambiguities can be determined mathematically in a case-by-case fashion. When known sets of Euler parameters are inserted into Equations 2 through 4 and yield identical scattering matrices, those sets constitute a scattering situation with unavoidable Euler ambiguities. Although the ambiguities are mathematically unavoidable, they can be shown to be physically meaningless. A simple redefinition of the Euler parameters for these special cases removes the ambiguities while still maintaining the physical relevance of the Euler transform.

For example, the sets of Euler parameters defined to have complete symmetry (τ=0°), a single bounce (υ=0°), no polarizability (γ=45°), 50% reflectivity (m=.5), and a certain orientation angle ($\psi=\psi_0$) are inserted into Equations 2-4. The resulting scattering matrices for this case turn out to be

$$S=\begin{bmatrix} .5 & 0 \\ 0 & .5 \end{bmatrix} \quad \text{when} \quad \tau=0°,\ \upsilon=0°,\ \gamma=45°,\ m=.5,\ \psi=\psi_0 \tag{15}$$

The resulting scattering matrices are identical regardless of the orientation angle used. In this way, the scattering matrix in Equation 15 has been identified to contain a complete ψ ambiguity. If this ambiguity is left unaddressed in practice, the transform equations will yield an unpredictable orientation angle that is dependent only on numerical machine error. From a physical standpoint, however, the above matrix is known to represent an isotropically curved surface such as a sphere. Physically, the orientation angle ψ of a sphere has no meaning, thus we are free to assign it an arbitrary value without degrading the physical meaning of the Euler parameters. Though the value to be assigned is arbitrary, a convention should be adopted and consistently applied to ensure reliable ISAR Euler image comparisons. In a similar way to this example case, all ambiguities can be identified and dealt with.

In order to create an optimized Euler transform, all of the possible Euler parameter ambiguities were identified, redefined, and removed. The identifications were accomplished by computing the scattering matrix for every possible set of Euler parameters, to within 1° increments, and finding all those scattering matrices that are identical. There were found to be 41 special cases where ambiguities arise and must be redefined. A handful of ambiguities and their redefinitions are presented in Table 1.

Ambiguous Sets				Scattering Matrix	Redefined Set				Description
γ	ψ	τ	ν		γ	ψ	τ	ν	
0	+-90	0	all	$\begin{bmatrix} 0 & 0 \\ 0 & d \end{bmatrix}$	0	90	0	0	wire at 90 deg
0	0	0	all	$\begin{bmatrix} a & 0 \\ 0 & 0 \end{bmatrix}$	0	0	0	0	wire at 0 deg
45	all	0	0	$\begin{bmatrix} a & 0 \\ 0 & a \end{bmatrix}$	45	0	0	0	flatplate, sphere
0	all	-45	all	$\begin{bmatrix} -ia & a \\ a & ia \end{bmatrix}$	0	0	-45	0	positive helix
0	-45	0	all	$\begin{bmatrix} -a & a \\ a & -a \end{bmatrix}$	0	-45	0	0	wire at -45 deg
0	all	45	all	$\begin{bmatrix} ia & a \\ a & -ia \end{bmatrix}$	0	0	45	0	negative helix

Table 1. A Few Ambiguous Euler Parameter Sets And Their Redefinitions

When all of the redefined Euler values for the special cases are combined with the standard transform equations (Equations 9, 10, 11, 13, 14) for the non-special cases, an optimized Euler transform is established. This optimized transform is able to more accurately and meaningfully image targets in Euler parameter space. A sample set of optimized ISAR Euler images is presented in Figure 1.

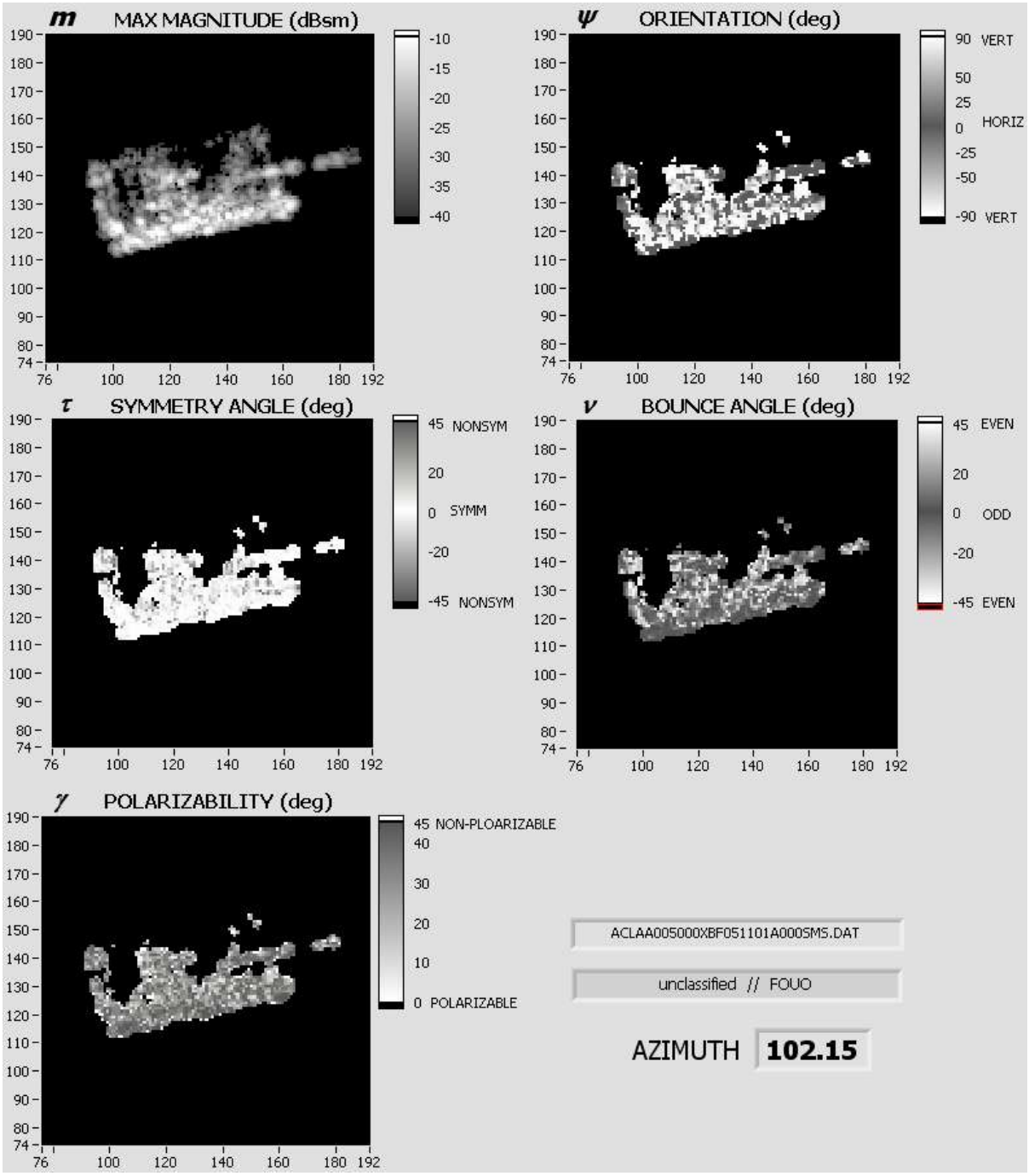

Figure 1. ISAR Images in Optimized Euler Parameter Space of the T-72BK Tank Fingerprint

4. CHARACTERIZATION OF NON-PERSISTENT SCATTERERS

Even after Euler parameter ambiguities have been removed, the reproducibility of ISAR Euler signatures is still degraded by the saturation of the image space by non-persistent scatterer. Scatterers that fluctuate rapidly for small changes in azimuthal look angle are considered non-persistent and lead to this degradation. The non-persistence of scatterer pixels is believed to be a result of multiple dominant scatters occupying the same pixel. It is hoped that the establishment of this hypothesis through the characterization of the non-persistent scatters will lead to better optimization of the Euler transform.

A scattering target can be represented conceptually as a collection of points in space known as scattering centers or scatterers for which there is significant reflectivity and for which the full scattering matrix can be known. The formation of an ISAR image of the target involves dividing space into a grid of resolution cells, or pixels. The scattering matrix values for each pixel are a complex sum of all of the scatterers contained in the pixel. Traditionally, each pixel is assumed to contain only one dominant scatterer, and thus the image is a faithful physical representation of the scattering target. In reality, many scatterers occupy the same image pixel but are at slightly different positions in space, thus the complex sum of their scattering matrices is naturally dependent on small changes in look angle. Therefore the non-persistence of certain pixels is hypothesized to be a result of this multiple-scatterer situation. The veracity of this hypothesis and the characterization of the non-persistent scatterer pixels can be established by comparing the persistence and reproducibility of the Euler parameters at different resolutions. If the non-persistence and degradation of the Euler parameters is a result of the multiple-scatterer summing within each pixel, then higher resolutions should better divide up the scatters into separate pixels and thus improve the persistence and reproducibility.

While persistence and reproducibility are mainly dependent on the specifics of the target's shape and complexity, their values as a function of resolution should exhibit the same general improvement trends if the multiple-scatterer concept is correct. For this purpose, three distinct targets of varying complexity were chosen and imaged at varying resolutions. The first target chosen was Slicy (Figure 2), a simple combination of flat surfaces and cylinders. The second target chosen, named Simulator (Figure 3), represents a middle level of complexity and is a general tank shape with small features removed. The third target investigated was a T-72M1 (Figure 4) which displays great complexity.

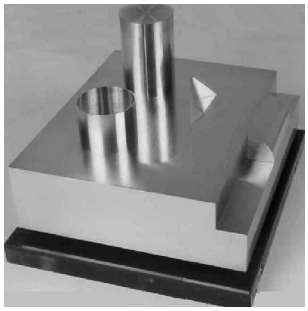

Figure 2. Slicy

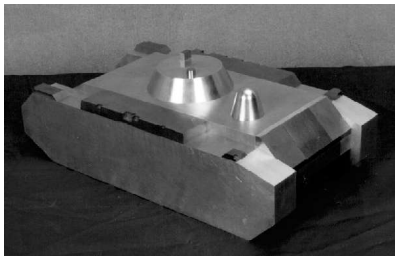

Figure 3. Simulator

Figure 4. T-72M1

To measure the reproducibility versus resolution, each target was measured twice and imaged in optimized Euler parameter space for each resolution. Each measurement consists of 360 Euler parameter image sets, one for each degree of look angle covering the full 360° sweep. The reproducibility error was measured between two images of corresponding azimuths and resolutions using a average difference method. The results were then averaged over azimuth to give an reproducibility error for each resolution, measured in Average Percent Difference (APD). The results are plotted for Slicy (Figure 5), Simulator (Figure 6), and the T-72 (Figure 7).

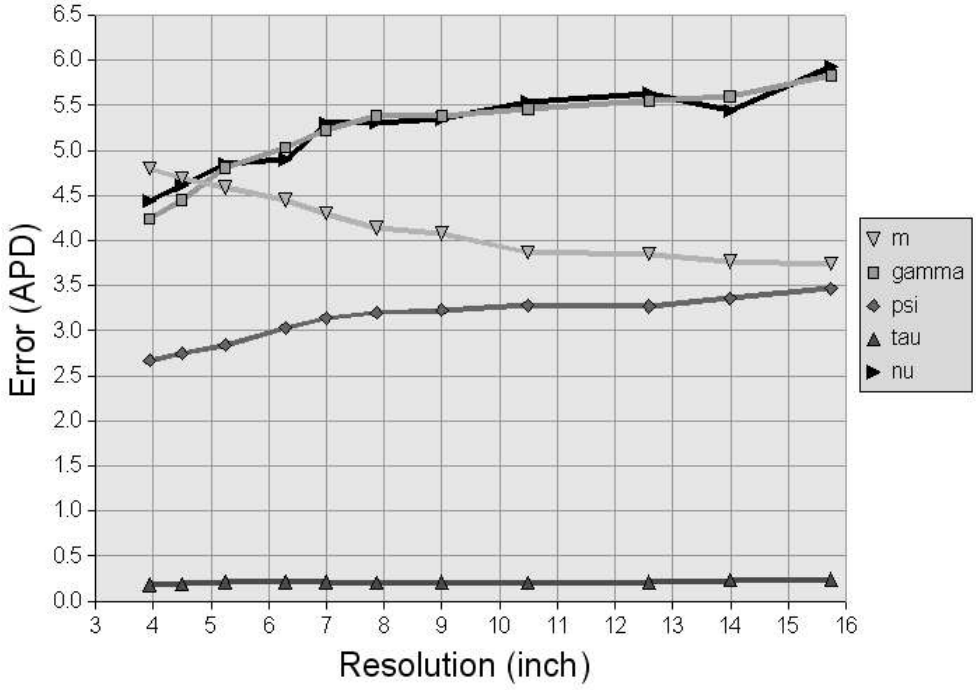

Figure 5. Slicy Target, Reproducibility Error vs. Imaging Resolution

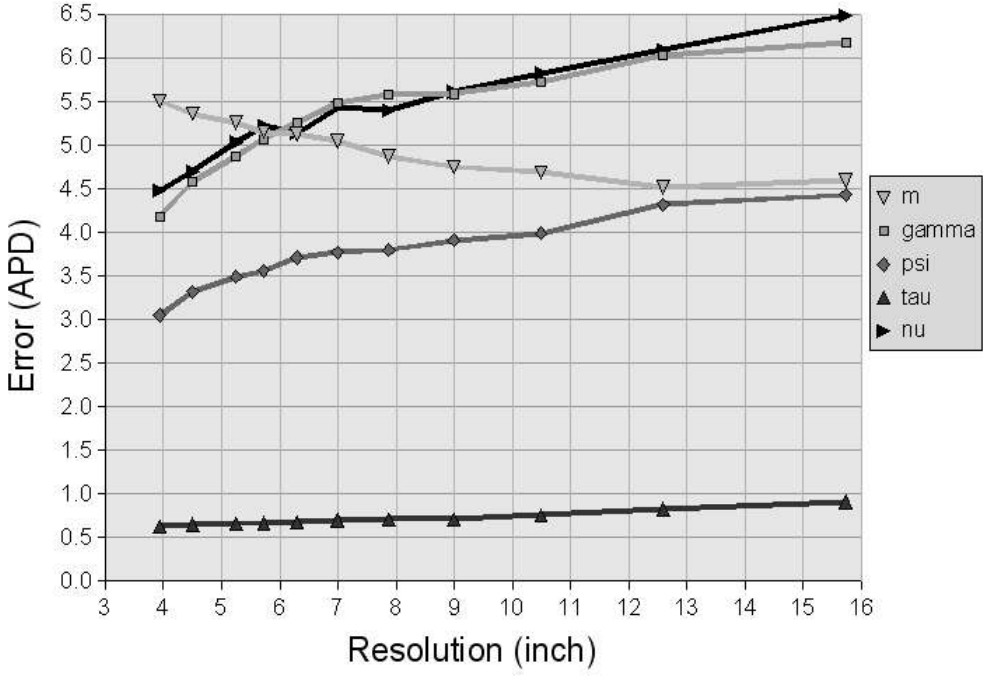

Figure 6. Simulator Target, Reproducibility Error vs. Imaging Resolution

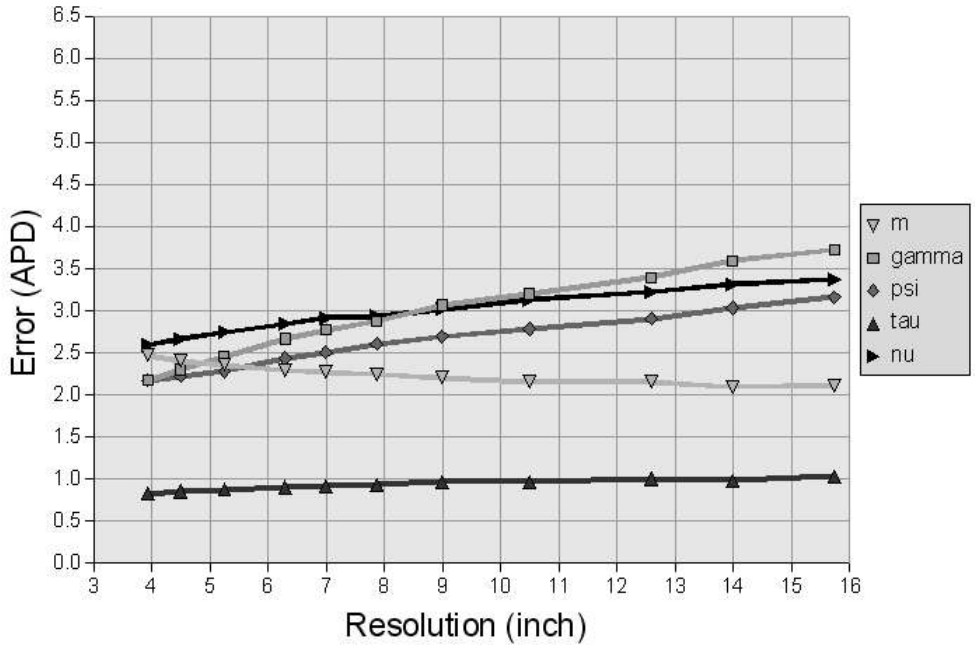

Figure 7. T-72 Target, Reproducibility Error vs. Imaging Resolution

Except for the maximum magnitude parameter *m*, the results are as expected in each case. Each parameter for each target demonstrates the general trend that as the pixel size decreases, fewer pixels contain multiple scatterers and thus the error diminishes. These results show that the presence of multiple-scatterer pixels is the cause of parameter degradation.

The *m* parameter shows the opposite resolution trends from what is expected, but this trend can be understood to be correct because *m* is a magnitude parameter while the others are angle parameters. Magnitude parameters are not as sensitive by nature to small phase differences in a complex sum, as arises when multiple scatterers are at slightly different locations but are still registered in the same pixel.

To measure the persistence versus resolution, each target was imaged in .2° look angle increments over the full 360° sweep. Each image was rotated back in azimuth by the amount of its look angle, which essentially made the target stationary in the sequence of images while the radar stepped through the full azimuthal circle. This series of back-rotations ensured that physical objects on the target remained in the same pixel throughout the image sequence instead of rotating through the typical path. The persistence of each scatterer in look angle could than be measured as the persistence of the same pixel throughout the image sequence. The pixel persistence was measured as the extent in images for which the pixel remained within 15% of its original value. The resulting persistence value was then averaged over all of the persistence scatterer swaths in the full 360° azimuth image sequence, which was then plotted versus resolution. The persistence results are given for Slicy (Figure 8), the Simulator (Figure 9), and the T-72 (Figure 10).

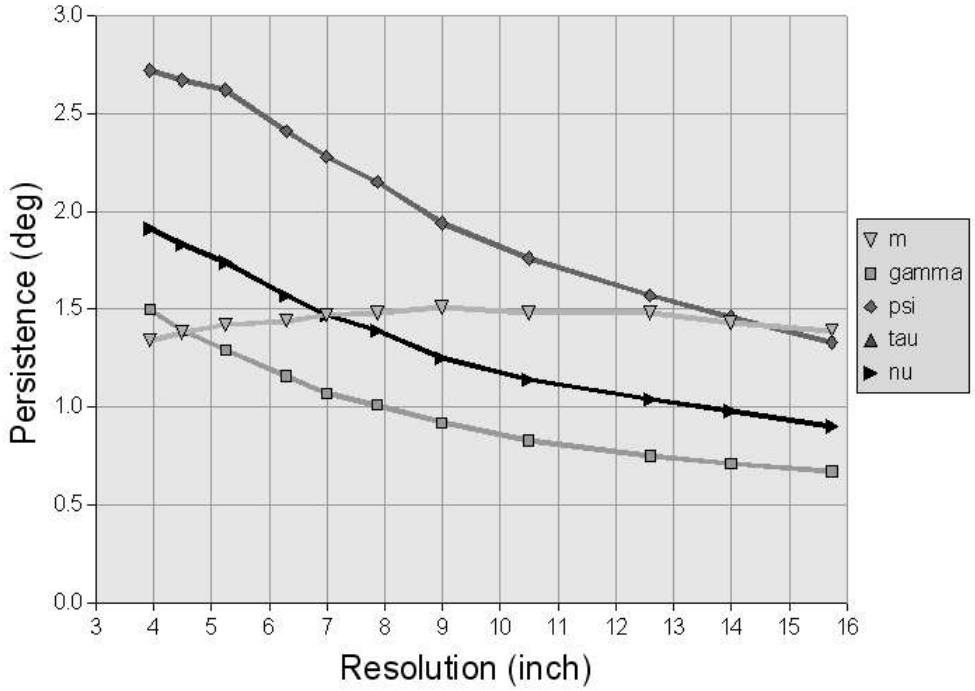

Figure 8. Slicy Target, Persistence vs. Imaging Resolution

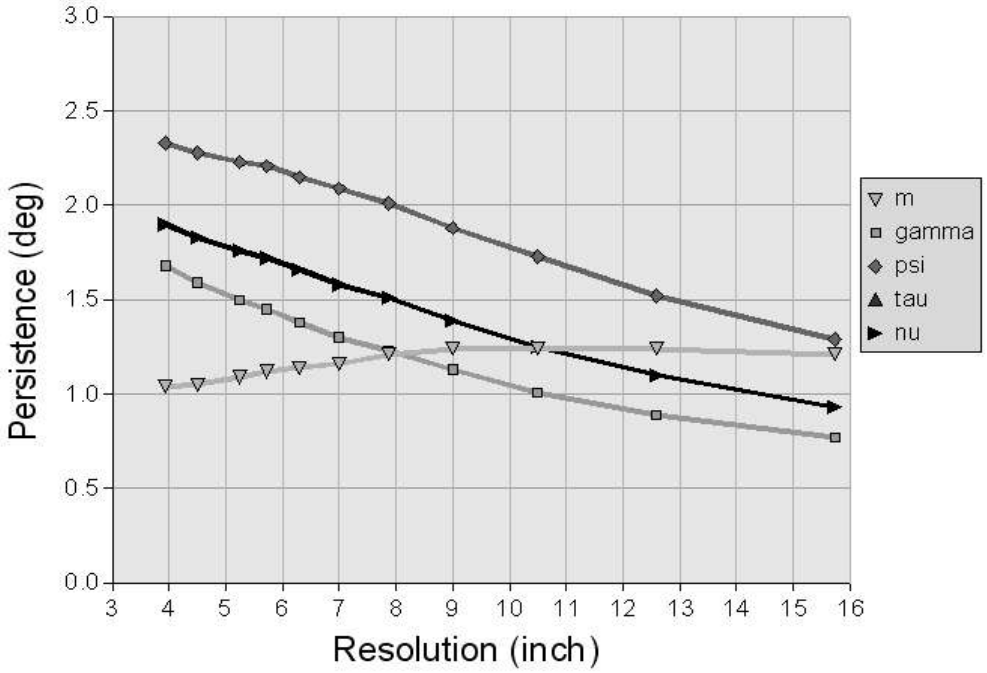

Figure 9. Simulator Target, Persistence vs. Imaging Resolution

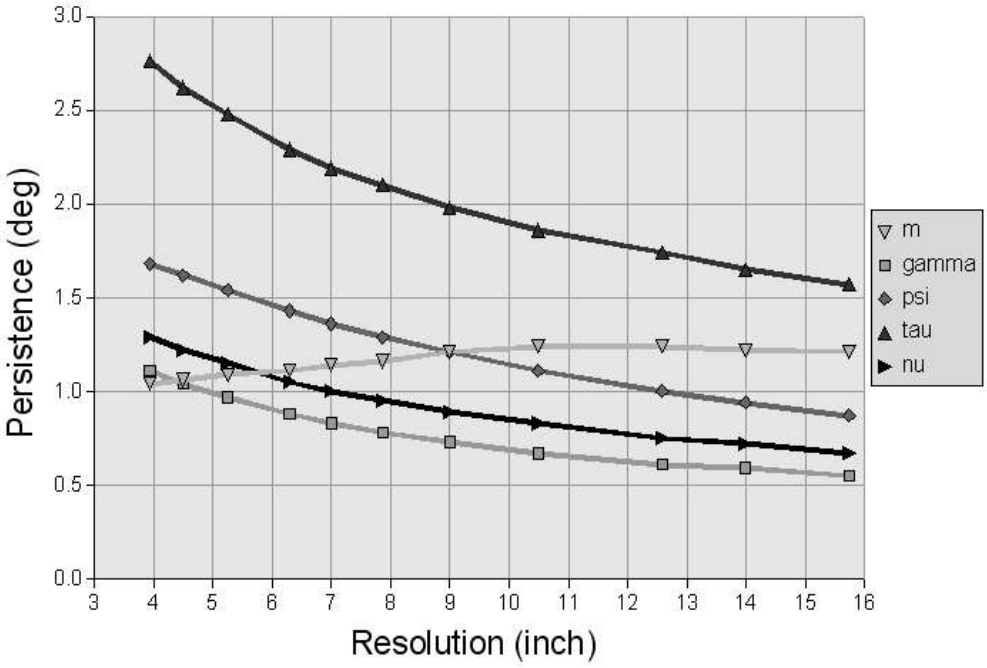

Figure 10. T-72 Target, Persistence vs. Imaging Resolution

The trends are again as expected for each parameter except *m*. For each target and each parameter except *m*, smaller pixel sizes are found to improve the azimuthal persistence of the scatterers. These results further support the claim that persistence and thus Euler parameter accuracy is degraded by the multiple-scatterer pixels.

The parameter *m* again shows the opposite trend as expected, which can be understood for the same reasons as stated above. It should also be noted that for Slicy and Simulator, the symmetry angle trends have been omitted. This ommission is because those particular targets are so symmetrical that the scatterers bleed together in symmetry images, making any measurement of symmetry angle persistence meaningless.

5.0 CONCLUSIONS

The Euler transform equations have been derived in a way that minimizes ambiguities using the Kennaugh matrix. A detailed analysis of the physical meaning of the parameter ambiguities has allowed the removal of the ambiguities through a case-by-case redefinition, and thus established an optimized Euler transform. Lastly, the reproducibility and persistence versus resolution trends have shown that multiple-scatterer pixels are indeed the cause of non-persistence and parameter degradation. It is hoped that in the future this characterization will allow for the isolation of more persistent and reliable scatters to improve target classification.

REFERENCES

1. M. N. Cohen, "Variability of ultrahigh-range-resolution radar profiles and some implications for target recognition", SPIE Vol. 1699, 1992.

2. Y. Le Helloco, L. Priou, B. Uguen, G. Chassay, "A study of the desying process of a radar target applied to a critical analysis of the meaning and the sensibility of some measured Huynen parameters", *Microwave and Optical Technology Letters*, Vol. 14, Issue 3 , 1998**.**

3. Jason C. Dickinson, Thomas M. Goyette, and Jerry Waldman,"High Resolution Imaging using 325GHz and 1.5THz Transceivers", *Fifteenth International Symposium on Space Terahertz Technology (STT2004)*, Northampton, MA, 2004.

4. R. H. Giles, W. T. Kersey, L. C. Perkins and J. Waldman,"A Variability Study of Ka-Band HRR Polarimetric Signatures on Eleven T-72 Tanks", *SPIE*, April 1998.

5. M. Coulombe, J. Waldman, R. Giles, A. Gatesman, T. Goyette, and W. Nixon,"Submillimeter-Wave Polarimetric Compact Ranges for Scale-Model Radar Measurements", *IEEE MTT-S International Microwave Symposium,* Seattle, Washington, 2002.

6. R.H. Giles, W.T. Kersey, M.S. McFarlin, H.J. Neilson, R. Finley and W.E. Nixon,**"**A Study of Target Variability and Exact Signature Reproduction Requirements for Ka-Band Radar Data", *SPIE*, April 2001.

7. L. Autonne, Sur les matrices hypohermitiennes et sur les matrices unitaires, *Annales de l'Universite de Lyon, Nouvelle Serie I, Fasc. 38,* 1-77, 1915.

8. E. M. Kennaugh, "Polarization Properties of Radar Reflections", MSc Thesis, Ohio State University, Columbus, OH, 1952.

9. J. R. Huynen, "Phenomenological Theory of Radar Targets," Ph.D. dissertation, Drukkerij Bronder-Offset N.V. Rotterdam, 1970

10. J. R. Huynen, "A Revisitation of the Phenomological Approach with Applications to Radar Target Decomposition," University of Illinois at Chicago, Chicago, MA, 1982.